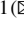







Heat and Mass Transfer in the Freezing Soils

Assel Sarsembayeva¹  , Askar Zhussupbekov¹ , and Philip Collins² 

¹ The L.N. Gumilyov Eurasian National University, Nur-Sultan 010008, Kazakhstan

² Brunel University London, London UB8 3PN, UK

Abstract. The moisture mass transfer in a gaseous state was previously widely neglected in the exploration of frost heave. The widespread model of coupled heat and water transfer allowed for detailed calculation and estimation of moisture migration by using the numerical methods. However, it could not explain the driving forces and physical nature. In this research, the significantly modified testing method, including the slow freezing techniques and longer samples lengths, was presented, as is an effective way to evaluate the impact of freeze-thaw cycles on soils. The moisture mass transfer in a state of vapour flow was considered during unidirectional freezing on the example of the conducted laboratory testing. The obtained results have improved understanding of the heat and mass transfer phenomenon during the unidirectional freezing of soils. The conceptual model for frost heave in soils was developed based on the vapour mass transfer. The algorithm of vapour flow calculation in unsaturated soils was presented using fundamental thermodynamic equations.

Keywords: Freeze-thaw test · Laboratory testing · Vapour mass transfer

1 Introduction

The subbases and subsoils of the structures in cold countries are subject to the frost heave due to increased thermal conductivity, disruption of natural moisture circulation as well as dynamic loading and application of de-icing chemicals in the winter months. The freezing rate in the highway structure is more rapid, and the temperature distribution is lower than that of adjacent roadside soils [1–3]. According to [4], the convective heat fluxes can lead to a significant change of the temperature field in highway subsoils and must be accounted for in road design and in the prognosis of subsoils' temperature distribution. Junwei et al. found that the maximum influencing depth for temperature fields under the embankments was over 8 m [5]. Observation of the temperature distribution during the freeze-thaw period on the local highways in Kazakhstan was performed by Teltayev and other researchers [6, 7].

Formation of frost heave within freezing soil is necessarily accompanied by moisture redistribution and heat transfer. Most of the studies were performed in the laboratory condition. Laboratory approaches benefit from better technical control and the ability to set the initial parameters of the soil sample, such as the temperature control plates and freezing rate, as well as being able to adjust these parameters during monitoring. The length of the samples mostly ranged from 15 cm to 20 cm or less [8] and rarely

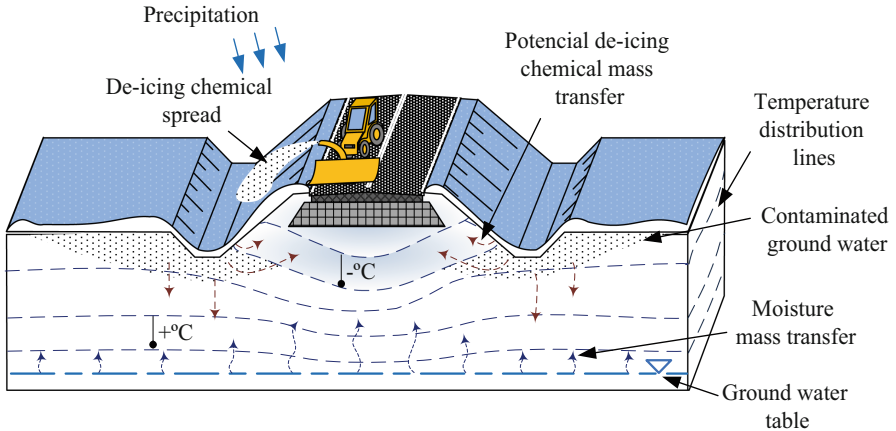


Fig. 1. Mass transfer under the highway pavement in seasonally freezing soils.

longer [9, 10]. The number of cycles is usually two, although in studies for mechanical properties, there might be more [11, 12]. Ming and Li (2015) presented an inverse relationship between the water influx and freezing rate was investigated for different water content samples, and developed a coupled water and heat mass transfer model based on this relationship [13]. Individual testing models have been developed for exclusively saturated soils and eliminating the vapour phase [14].

Some of the experiments were conducted in an adapted triaxial cell, which allows measuring pore pressure, the major principal stress σ_1 in the vertical axis and radial minor principal stress σ_3 [15, 16] tested frozen saline silt under triaxial compression and at close to freezing temperatures, $-3.9\text{ }^\circ\text{C}$ and $-2.4\text{ }^\circ\text{C}$ [16]. Conducting the freeze-thaw cycles in the triaxial cell allowed them to observe a relationship between the strain rate and freezing temperature. However, triaxial cell tests enable a contemporaneous mechanical loading of only one soil sample at a time. The size of the tested sample is also restricted by the size of the test cell.

The classical view of frost heave involved mainly considering water-ice interaction and their migration, while the vapour component in soils was widely ignored. Moreover, the widespread model of coupled heat and water transfer allowed for detailed calculation and estimation of moisture migration by using the numerical methods. However, it could not explain the driving forces and physical nature. Nevertheless, the developed methods and approaches formed the basis of the breakthrough of numerical methods and, moreover, achieved tolerable results in frost heave calculations and prognosis.

Vapour convection has been widely underestimated in geotechnics up to the present day, and its calculation has been generally neglected in moisture transfer modeling [17]. To fill this gap in the knowledge it was decided to conduct a cyclical freeze-thaw experiment with a modified testing method, which was adapted to allow for the close examination of mass transfer in the freezing subsoils of highways.

2 Method

The laboratory method with freeze-thaw cycles in ‘open system’ was based on ASTM D 5918-06 Standard. However, some principle changes were made, and the length of the samples was increased to 0.5 m in order to improve the observation of the temperature gradient during freeze-thaw cycles (see Fig. 2). The freezing rate was conducted with 2 °C temperature reduction of surface temperature per day. The increased capacity environmental chamber was designed and built to enable the testing of nine soil columns at a time, each of 10 cm diameter and of lengths 50 cm and up to 1 m.

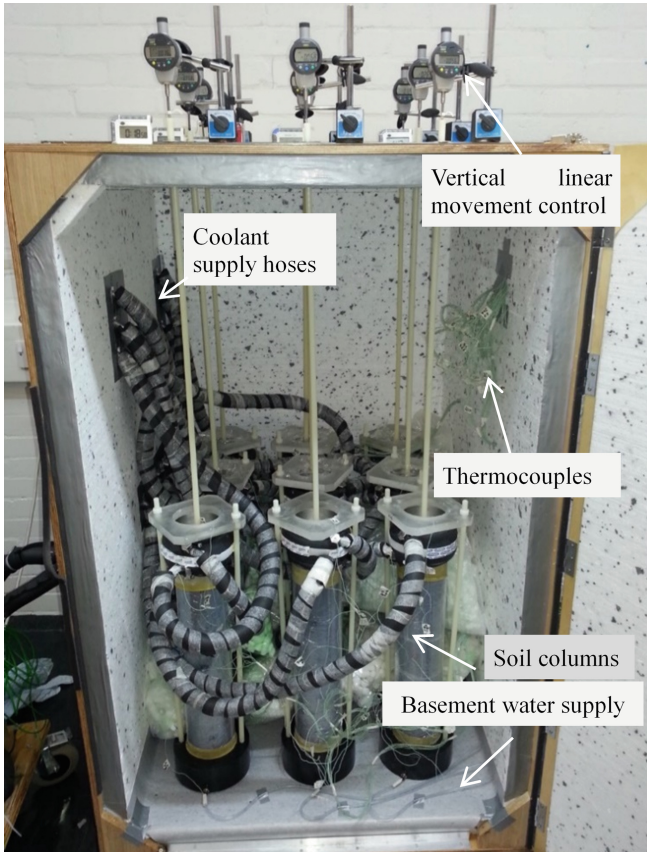


Fig. 2. Environmental chamber.

2.1 Sample Preparation

Each soil column was equipped with a basement water supply from the reservoir and an air tap fitted at 10 cm above the base, allowing the excess air pressure to be released as the column filled with water. The bottom 5 cm of the test soil sample was kept saturated during the test, while the other 45 cm remained in an unsaturated condition. To provide

the uniform distribution of water supply over the sample cross section, the feed was provided via a 5 cm thick fine sand filter layer at the base of the column (see Fig. 3). The soil samples were prepared to simulate the engineering properties of soil from Astana, Kazakhstan. Local soils of the area presented the ancient sedimentary rocks, which comprise irregular thicknesses of residual layers and alluvium depositions, according to borehole data from Karaganda GIIZ [18].

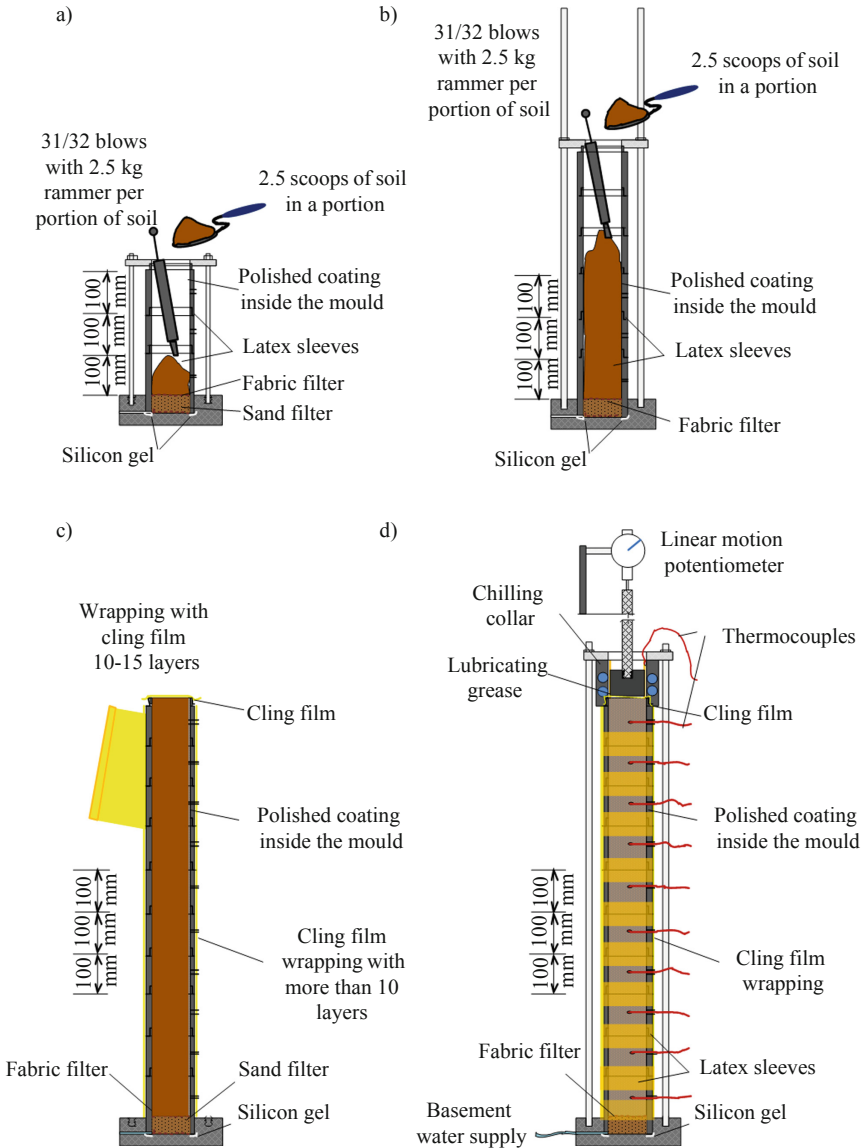


Fig. 3. Sample preparation.

Table 1. Initial characteristics of the soil.

Characteristic	Symbol	Unit	Value	Annotation
Initial moisture content	W	%	17.2	According to 95% max. dry density – moisture content relationship
Angle of internal friction	φ	°	24.1°	CD direct shear test, moisture content $W = 17.2\%$
Cohesion	C	kN/m ²	10	
Particle density	ρ_s	Mg/m ³	2.615	Soil mixture by mass: 50% sand and 50% kaolinite
Average dry density before freezing cycle	ρ_d	Mg/m ³	1.814 ± 0.012	BS Light compaction test operating with 2.5 kg rammer. The mechanical energy applied to the soil is 596 kJ/m ³
Initially bulk density at the beginning of the test	ρ	Mg/m ³	2.128 ± 0.015	
Uniformity coefficient	C_u	–	2.4	Uniformly-graded sand
Coefficient of curvature	C_c	–	3.65	
Activity of clays	A	–	0.25	Inactive clays
Liquid limit	w_L	%	37.18	CI – Medium plasticity cone penetrometer test used
Plastic limit	w_P	%	23.77	Fraction of soil sample passed through 0.425 mm sieve
Average linear shrinkage	L_S	%	5	
Plasticity index	PI	%	13	

The compaction of the soil was in accordance with BS1377-1:1990. The number of blows applied per 10 cm diameter and 10 cm length section was corresponding to the effort. The samples were compacted with increasing order of dry density between the columns. To obtain the uniform distribution of the material within the volume, an equal amount of soil (by scoops) was compacted with the same energy effort over the sample length. The achieved dry density in column #1 was equal to 1.178 Mg/m³. The density of each further column increased. Columns 9 was compacted with maximum dry density corresponding to a 17.2% moisture content. A standard proctor test was conducted with a 2.5 kg rammer in the assembled mold for the freeze-thaw cycles. 63 blows per section volume, each being subdivided into two layers of 5 cm and compacted with 31/32 blows by rotation. The air void content under the applied compaction procedure was close to zero, and the soil sample was very close to the fully saturated state. The initial mass, volume and density parameters are presented in Table 2.

The testing process consisted of two freezing-thawing cycles. After 24–36 h of the conditioning period, the chilling collars at the top of the soil sample were cooled down to 3 °C. The moisture supply temperature at the base of the soil columns was kept stable at +4 °C. After the conditioning period, the circulated coolant temperature at the temperature control machine was reduced to –3 °C and subsequently was dropped daily

Table 2. Density distribution within the soil samples

Column number	Average volume in a mould, cm ³	Weight of assembled mould with sand filter layer, g	Weight of the compacted sample in the mould before test, g	Weight of soil before test, g	Dry density before the test, Mg/m ³
#1	3,966	4,121	9,602	1.382	1.178
#2	3,966	4,105	10,160	1.527	1.302
#3	3,966	4,117	10,372	1.577	1.345
#4	3,966	4,120	10,961	1.725	1.471
#5	3,966	4,095	11,201	1.792	1.527
#6	3,966	4,115	11,591	1.885	1.607
#7	3,966	4,110	11,792	1.937	1.651
#8	3,966	4,114	12,466	2.106	1.795
#9	3,966	4,122	12,485	2.109	1.798

by a further 2 °C. It should be noted that the heat loss between the temperature control unit and the cooling ring on the top of the soil sample was approximately 2–3 °C. The red stepped line in Fig. 4 represents the temperature at the temperature control unit, while the temperature reaction of the soil surface is shown as a flowing line. The freezing rate of the soil sample was dropped by 2 °C every 24 h for 12 days and reduced down to –23 °C at the temperature control unit. When the coolant supply temperature had decreased to –23 °C, it was held there for the next 24 h. Afterward, all the cooling system was switched off, and the environmental chamber was slowly returned to room temperature through natural thawing.

2.2 Post-freeze-Thaw Sampling and Testing

After the end of the second freezing cycle, the soil columns were unplugged from all monitoring and fixing elements, removed from the environmental chamber and weighed immediately in the frozen state. After that, each column was positioned horizontally to avoid the possible draining of melting moisture in a longitudinal direction. The soil columns were disassembled in-ring sections and sampled for moisture content determination every 1 cm in the top and the bottom ring sections and every 10 cm in the middle lengths of the soils. The sampling procedure was generally carried out the same day before the soil started to thaw in order to prevent moisture redistribution or structure change during melting.

The moisture content was found according to standard BS 1377-4:1990 by weight difference of the wet and oven-dried sample at 105 °C for a 24 h period. The total moisture content included that attributed to the mass of ice lenses and the mass of water in a liquid condition. The top 10 cm section was sampled every 1 cm due to the increased

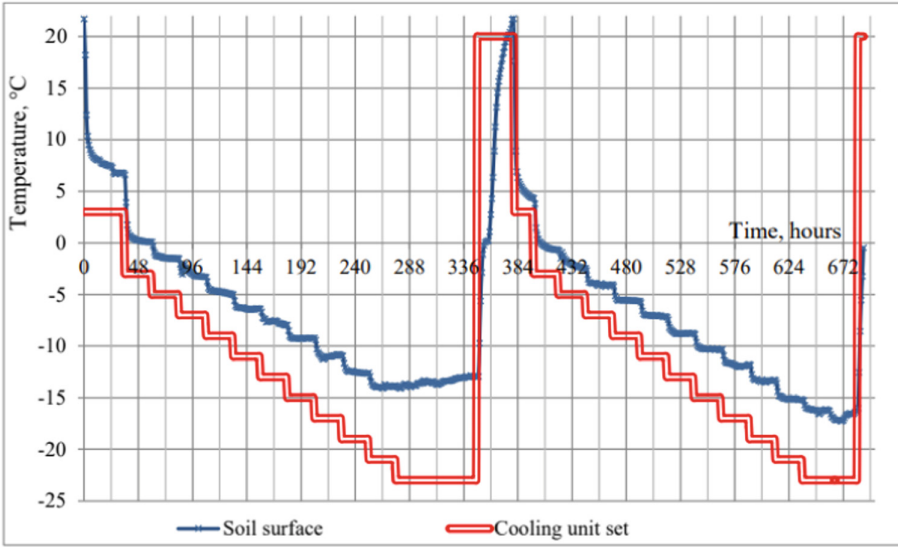


Fig. 4. The cooling unit sets the temperature and the corresponding temperature on the soil surface.

ice lens formation and the anisotropic structure, while the lower part of the soil column was only sampled every 10 cm, mainly at the junctions of the mold sections.

2.3 Calculation of the Vapour Mass Transfer in Unsaturated Freezing Soils

The algorithm for calculation of vapour mass transfer includes determination of volumetric and mass constituents of soils such as water, soil particles, vapour. Porosity and the volume of air are the crucial characteristics for the vapour mass transfer in freezing soils (Fig. 5).

The heat change Q in a mold section over the time t is found as the sum of the cooling heat and the latent heat during the phase transfer:

$$Q \cdot t = Q_1 + Q_2 \tag{1}$$

where, Q_1 is heat energy used for cooling the vapour mass to the temperature ΔT ; and Q_2 is heat energy is used for phase transfer.

$$Q_1 = m_{vapour, t_i} \cdot C \cdot \Delta T \tag{2}$$

where m_{vapour, t_1} a mass of vapour at the starting time t_1 , g; C – specific heat of vapour passing through the cumulative air voids cross-section, $J/kg \cdot ^\circ C$; ΔT – temperature change, $^\circ C$; and t – time interval, h.

If part gravitational water remains in the unfrozen condition, the mass of vapour is found by Eq. (2). The density of the vapour is calculated for each period of time, corresponding to the temperature and saturated vapour pressure:

$$\rho_{vapour, t_i} = \frac{m_{vapour, t_i}}{V_{air, t_i}} \tag{3}$$

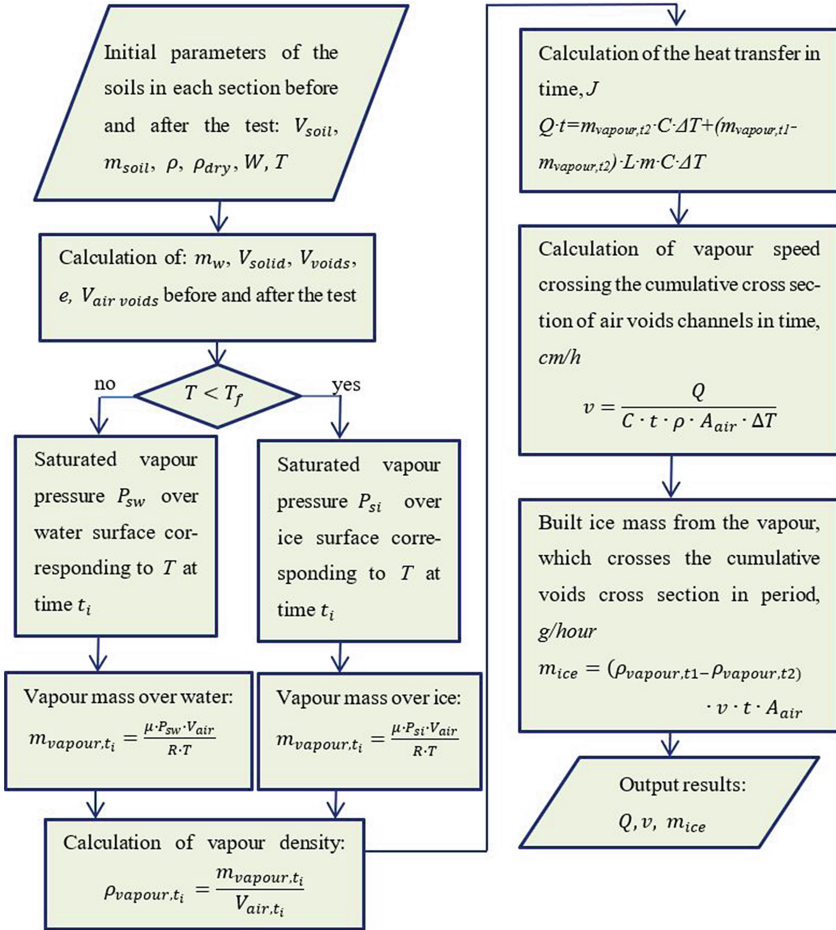


Fig. 5. Algorithm for the vapour mass transfer calculation.

where, ρ_{vapour,t_i} - vapour density for period of time, g/cm^3 .

Heat energy for the phase transfer includes the latent heat for the condensation and solidification of the vapour mass difference at the beginning τ_1 and end time τ_2 of the calculation period.

$$Q_2 = (m_{vapour,1} - m_{vapour,2}) \cdot L \quad (4)$$

where, $m_{vapour,2}$ – mass of the vapour at the end period t_2 ; L – is a total latent heat $L = L_1 + L_2$, where L_1 - specific latent heat for condensation $L_1 = 2.3 \cdot 10^6$ J/kg and L_2 - specific latent heat for solidification $L_2 = 0.335 \cdot 10^6$ J/kg of 1 kg of water.

The volume of vapour V_{vapour} is equal to the speed of vapour passing through the air voids' cross-section A over the time t :

$$V_{vapour} = v \cdot t \cdot A_{air\ voids} \quad (5)$$

where, v – an average speed of vapour, cm/h; and $A_{air\ voids}$ – cumulative section cross of the air voids' $A_{air\ voids} = \frac{\pi \cdot d_a^2}{4}$, cm^2 , corresponding to the porosity coefficient and moisture content (see Fig. 6).

Substituting the V_{vapour} in Eq. (2) the vapour speed is found at the starting time and at the end:

$$v_{vapour} = \frac{4Q}{C \cdot \rho \cdot \pi \cdot d_a^2 \cdot \Delta T \cdot t} = \frac{Q}{C \cdot \rho \cdot A_{air} \cdot \Delta T \cdot t} \tag{6}$$

The mass of ice built from the vapour passing through the air voids channels in a 10 cm length mould section with a correspondent cumulative cross-section A_{air} and speed v over time t is calculated:

$$m_{ice} = \rho_{vapour} \cdot V_{air\ voids} = \rho_{vapour} \cdot v \cdot t \cdot A_{air} \tag{7}$$

where, m_{ice} is mass of built ice in grams; ρ_{vapour} is taken as an average density value of the vapour densities at the start and end time point, g/cm^3 .

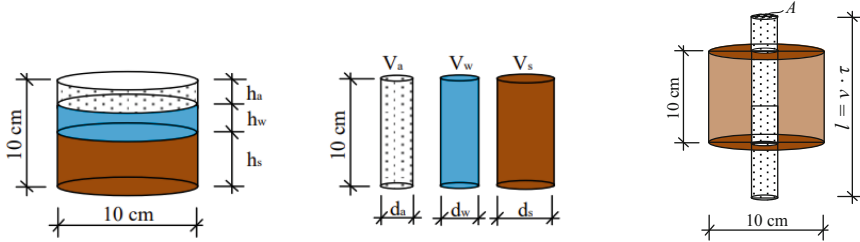


Fig. 6. Vapour rate passing through the cumulative air voids channel in the mold section over time t .

Here, it is assumed that the porosity coefficient of the sample remains constant during the calculation period. Consequently, the volume of the air voids and the cumulative cross-section of the air voids also remain constant. It should be noted that only heat consumed for the gas phase energy exchange was considered in this problem. The solid and liquid parts have also been cooled down with the heat withdrawn by the cooling machine. However, they are not counted because all the necessary energy exchange has been done by an automatic set of temperature controls.

The model is suitable for numerical solutions, like finite element analysis or a model similar to a coupled heat-water transfer, in terms of considering the vapour flow and taking into account the cross-section forces. The latent heat for the phase transitions and the dynamic change of the coefficient of porosity and air void volume also needs to be taken into account.

3 Results

The temperature distribution in the freeze-thaw test with a range of soil density did not obtain a steady pattern of freezing rate in terms of initial density. This is possible

because the freezing rate of $2\text{ }^{\circ}\text{C}$ per day provided sufficient time for uniform temperature distribution and stabilization of the temperature field across the range of soil densities. However, a deceleration of the freezing rate was noted in the second freezing cycle.

Figure 7 shows the time intervals when the temperature reached 0 , -5 and $-10\text{ }^{\circ}\text{C}$ for the part 15 cm from the top of each soil sample, during both the first and second freezing cycles. In column #1, $-5\text{ }^{\circ}\text{C}$ was registered at 15 cm depth from the soil surface after 147 h for the first freezing cycle, and this took 518 h in the second freezing cycle (Fig. 8).

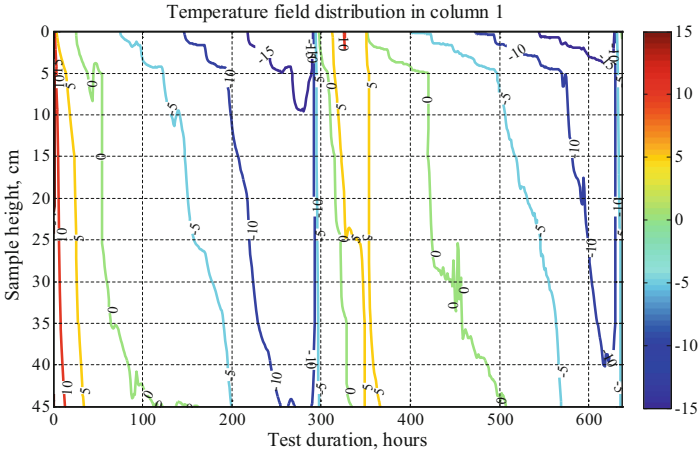


Fig. 7. Temperature field contours.

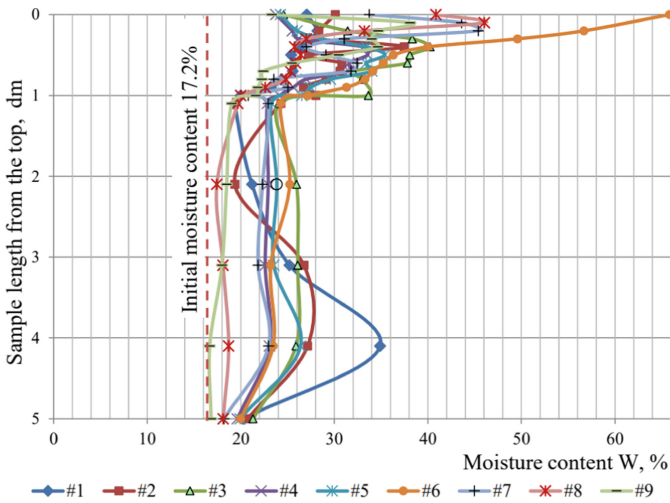


Fig. 8. Moisture intake during the freeze-thaw cycles of the soils in test with a deionized water supply and various densities.

In the top 10 cm layer, ice lens formation caused a highly irregular distribution of moisture, which was justified by the centimeter sampling. Since the groundwater supply table was quite shallow, at 45 cm depth, the moisture intake was higher than for Columns 8 and 9, where the water supply was located at 95 cm depth, and the soil samples were made with maximum dry density. For this reason, the moisture content between 15 and 45 cm from the soil surface was relatively stable and depended just on the density of the soil samples (Fig. 9).

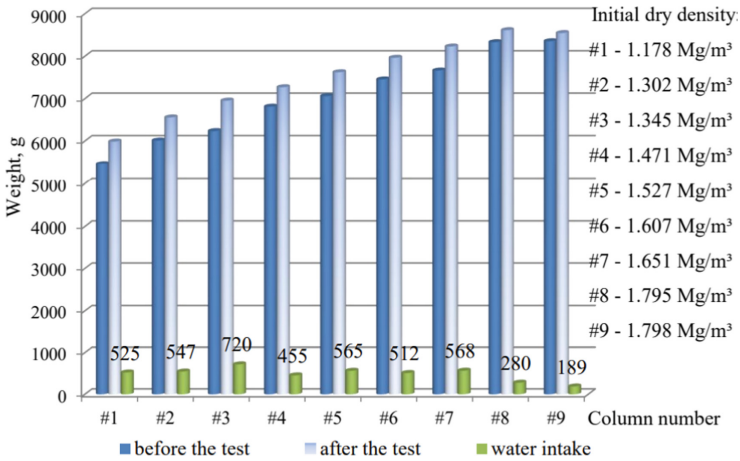


Fig. 9. Sample preparation.

According to the results, the moisture content represents advanced water intake in the loose soil, with a dry density range between 1.18–1.65 Mg/m³, compared to dense soils with a dry density 1.8 Mg/m³. With the exception of sample #4, in all the columns, the moisture content reached 24.5% or above by the end of the test. The reason for low moisture intakes in sample #4 could have been due to occasional violation of the water supply during the freeze-thaw test.

In freeze-thaw cycles test with a deionized water supply from the base, the maximum rates of frost heave were achieved in columns #7 and #8, where the dry density was close to the maximum value of 1.65–1.79 Mg/m³. While the loose soil samples, with dry density 1.18–1.47 Mg/m³, registered very weak heaving in the first cycle and consolidation or compression in the second cycle compared to the initial volume (Fig. 10).

In freeze-thaw tests with variable initial density packing, the sample with loose soils condensed during the freeze-thaw cycles, whilst the dense samples were loosened (see Fig. 11). Regarding sample length, the top layers were always loosened due to the high content of ice lenses formed at the cold front. The bulk density distribution by the column length is presented in Fig. 12. The columns with loose density were consolidated throughout the column length, with the most value in the lower parts of the samples. Whilst in the dense soil samples, only the 10 cm layer on top was loosened and had attracted a large amount of water to form ice lenses.

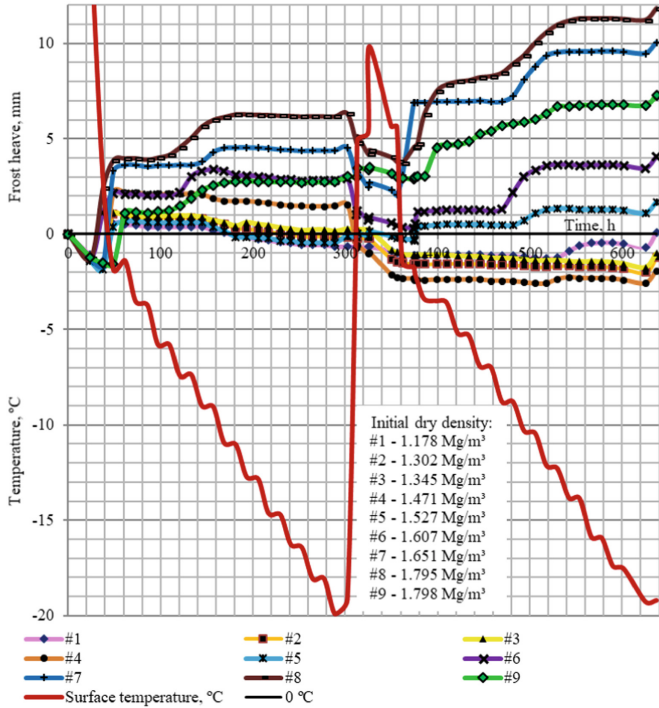


Fig. 10. Frost heave in the samples with varied densities.

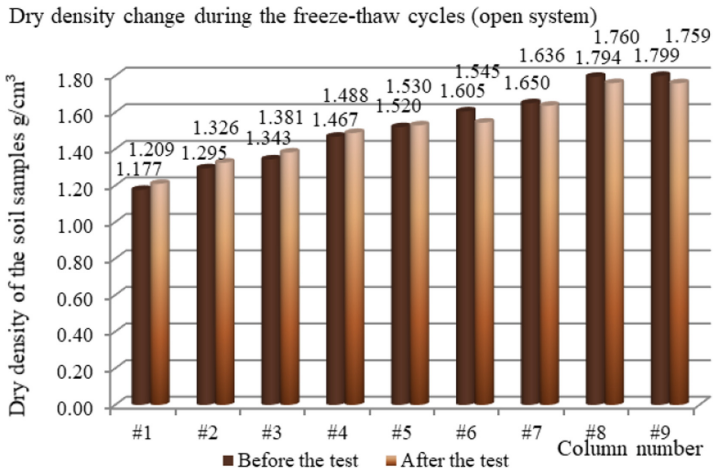


Fig. 11. General density change in the samples with variable dry density.

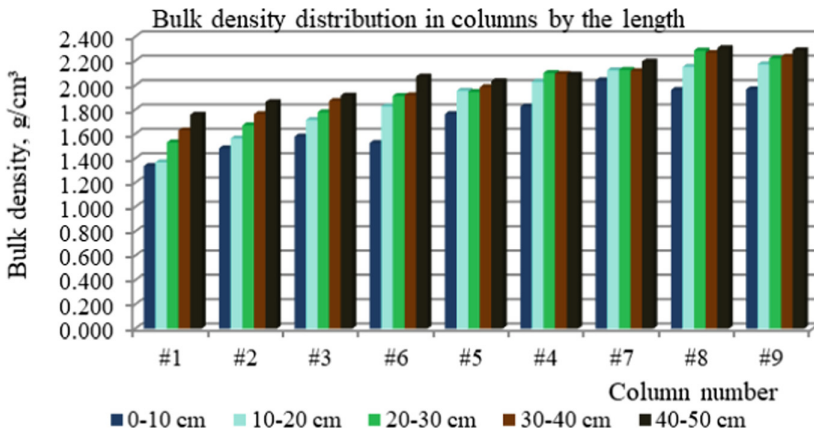


Fig. 12. Bulk density distribution by the column length

3.1 Determination of the Vapour Mass Transfer in Unsaturated Freezing Soils

The results of the density-moisture parameters before and after the freeze-thaw test are presented in Table 3. Here, under the “before test” title, the initial setting parameters at $t = 0$ h are presented. Whilst under the “after test” title, the data collected after two freeze-thaw cycles at $t = 636$ h are shown.

The period of time between 590 h and 614 h, which corresponded to the end of the second freezing cycle period, was considered for analyzing the mass transfer within the frozen soils. Sub-zero temperature distribution is presented in Tables 5a and 5b. The length of the soils sample was 50 cm, which was composed of five assembled mold sections, each 10 cm in length. Moreover, each of the sections had an overlay joint of 5 mm. Because the density varied from the loosest one in column #1 to the densest #8 and #9, it was decided to consider the mass moisture transfer in the unsaturated samples #1 and #7.

The mass and volume of the solid particles were believed to stay unchanged during the freeze-thaw cycles, while the moisture content and the volume of voids had been modified. The ice lenses formed mostly in the top section layer, which caused some linear deformation in the vertical direction and was taken into account only for the top section.

Further calculations were performed on top section #11 in soil column #1 for the time interval between 590 and 614 h (Table 4). The moisture content intake and its distribution over the sample length were set at the beginning and measured at the end of the two freeze-thaw cycles. Because the time slot was considered during the final freezing stage of the test, the moisture content distribution and correlated volumetric-density calculations have been performed according to the data presented in Table 1.

Table 3. Soil sample parameters before and after the freeze-thaw cycles.

Column	Weight of soil, g		Bulk density, average by sample length ρ , Mg/m ³		Moisture content, average by sample length W, %		Dry density, average by sample length ρ_{dry} , Mg/m ³		Void ratio, average by sample length e	
	Before	After test	Before test	After test	Before test	After test	Before	After test	Before	After test
#1	5,463	5,988	1.380	1.512	17.20	25.01	1.177	1.209	1.223	1.162
#2	6,012	6,559	1.519	1.660	17.20	25.23	1.295	1.326	1.020	0.972
#3	6,236	6,956	1.575	1.760	17.20	27.39	1.343	1.381	0.947	0.893
#4	7,452	7,964	1.883	1.842	17.20	23.78	1.605	1.488	0.629	0.604
#5	7,057	7,622	1.783	1.918	17.20	25.35	1.520	1.530	0.721	0.709
#6	6,813	7,068	1.721	1.994	17.20	29.07	1.467	1.545	0.782	0.907
#7	7,662	8,230	1.936	2.037	17.20	24.50	1.650	1.636	0.585	0.598
#8	8,332	8,612	2.105	2.124	17.20	20.70	1.794	1.760	0.457	0.486
#9	8,355	8,544	2.111	2.126	17.20	20.85	1.799	1.759	0.453	0.487

Table 4. Calculation of soil parameters for the 590–614 h time interval on the example of sample #1.

Sample section	Distance from the top surface, cm	Volume in a section, cm ³	Mass of solids, g	Mass of water, g	Mass of the soil in a section, g	Bulk density, Mg/m ³	Average moisture content W, %	Dry density, Mg/m ³
#11	0–10	819	969.2	245.59	1214.76	1.483	25.34	1.183
#12	10–20	785.4	923.0	187.28	1110.30	1.414	20.29	1.175
#13	20–30	785.0	923.0	214.14	1137.16	1.448	23.20	1.175
#14	30–40	785.4	923.0	277.37	1200.39	1.528	30.05	1.175
#15	40–50	785.4	923.0	254.75	1177.78	1.500	27.60	1.175

The results of moisture mass transfer calculations in column #5 are presented in Tables 6, 7a and 7b. The average bulk density of the soil at the end of freeze-thaw cycles was 1.89 g/cm³. The moisture content comprised 30% at the top section and 23–24% in the rest of the sample. The obtained ice mass formation rate was in the range of 6.18 ·

Table 5a. Calculation of the mass moisture transfer in the soils for sample #1

Sample section	Volume of solids, cm ³	Volume of voids, cm ³	Void ratio e	Volume of air, cm ³	Temperature at 590 h	Saturated vapour pressure over ice, P _{si} , Pa	Mass of vapour at 590, g	Density of the saturated vapour at 590 h, Mg/m ³
#11	370.62	448.46	1.21	180.55	-10.99	237.93	3.55 · 10⁻⁴	1.97 · 10⁻⁶
#12	352.97	432.43	1.23	228.13	-10.30	253.24	4.76 · 10 ⁻⁴	2.09 · 10 ⁻⁶
#13	352.97	432.43	1.23	198.83	-9.49	272.16	4.45 · 10 ⁻⁴	2.24 · 10 ⁻⁶
#14	352.97	432.43	1.23	129.85	-8.36	300.63	3.19 · 10 ⁻⁴	2.46 · 10 ⁻⁶
#15	352.97	432.43	1.23	154.52	-6.46	354.77	4.45 · 10 ⁻⁴	2.88 · 10 ⁻⁶

Table 5b. Calculation of the mass moisture transfer in the soils for sample #1 (continuation of Table 5a)

Sample section	Temperature at 614 h, °C	Saturated vapour pressure over ice, P _{si} , Pa	Mass of vapour at 614 h, g	The heat realised in 24 hours $Q \cdot t = m \cdot C \cdot \Delta T$, J	Vapour rate $v = 4 \cdot N / (C \cdot \rho \cdot \pi \cdot d^2 \cdot \Delta T)$, cm per 24 h	Vapour rate, cm/h	Build-up of ice mass between the period 590/614 h, g/hour
#11	-13.30	193.26	2.91 · 10⁻⁴	0.1702	9.008	0.375	2.67 · 10⁻⁶
#12	-12.60	205.98	3.91 · 10 ⁻⁴	0.2269	9.014	0.376	3.56 · 10 ⁻⁶
#13	-11.68	223.81	3.69 · 10 ⁻⁴	0.2016	9.067	0.378	3.16 · 10 ⁻⁶
#14	-10.43	250.35	2.68 · 10 ⁻⁴	0.1363	9.126	0.380	2.14 · 10 ⁻⁶
#15	-8.96	284.98	3.61 · 10 ⁻⁴	0.2237	8.956	0.373	3.51 · 10 ⁻⁶

Table 6. Calculation of soil parameters for the 590–614 h time interval for sample #5

Sample section	Distance from the top surface, cm	Volume in a section, cm ³	Mass of solids, g	Mass of water, g	Mass of the soil in a section, g	Bulk density, Mg/m ³	Average moisture content W per section, %	Dry density, Mg/m ³
#11	0–10	854.73	1251.96	374.086	1626.05	1.902	29.88	1.465
#12	10–20	785.40	1192.34	280.797	1473.14	1.876	23.55	1.518
#13	20–30	785.40	1192.34	282.347	1474.69	1.878	23.68	1.518
#14	30–40	785.40	1192.34	297.609	1489.95	1.897	24.96	1.518
#15	40–50	785.40	1192.34	276.147	1468.49	1.870	23.16	1.518

Table 7a. Calculation of the moisture mass transfer in the soils for sample #5

Sample section	Volume of solids, cm ³	Volume of voids, cm ³	Void ratio e	Volume of air, cm ³	Temperature at 590 h, °C	Saturated vapour pressure over ice, P _{si} , Pa	Mass of vapour at 590, g	Density of saturated vapour at 590 h, Mg/m ³
#11	478.76	375.97	0.79	0	−13.48	190.14	–	–
#12	455.96	329.44	0.72	23.12	−11.45	228.51	$4.37 \cdot 10^{-5}$	$1.89 \cdot 10^{-6}$
#13	455.96	329.44	0.72	21.43	−10.69	244.59	$4.33 \cdot 10^{-5}$	$2.02 \cdot 10^{-6}$
#14	455.96	329.44	0.72	4.78	−10.29	253.46	$9.99 \cdot 10^{-5}$	$2.09 \cdot 10^{-6}$
#15	455.96	329.44	0.72	28.20	−8.98	284.46	$6.58 \cdot 10^{-5}$	$2.33 \cdot 10^{-6}$

10^{-8} – $3.82 \cdot 10^{-7}$ g/h (Table 7b). In the top 10 cm layer by the initial time of the testing period 590 h, the soil had reached the fully saturated condition, and further mass transfer was implemented via hygroscopic water in a liquid state. Consequently, the vapour mass transfer calculation in the top section was not applicable from that moment onwards.

Table 7b. Calculation of the moisture mass transfer in the soils for sample #5 (continuation of Table 7a)

Sample section	Temperature at 614 h, °C	Saturated vapour pressure over ice, P _{si} , Pa	Mass of vapour at 614 h, g	The heat realised in 24 h $Q \cdot t = m \cdot C \cdot \Delta T$, J	Vapour rate $v = \frac{4}{\pi} \cdot \frac{N}{C \cdot \rho} \cdot d^2 \cdot \Delta T$, cm per 24 h	Vapour rate, cm/h	Build of ice mass between 590/614 h period, g/h
#11	-15.46	158.49	–	–	–	–	–
#12	-13.61	187.89	$3.63 \cdot 10^{-5}$	0.0199	9.066	0.378	$2.82 \cdot 10^{-7}$
#13	-12.83	201.65	$3.60 \cdot 10^{-5}$	0.0194	9.078	0.378	$2.76 \cdot 10^{-7}$
#14	-12.36	210.49	$8.36 \cdot 10^{-6}$	0.0043	9.113	0.380	$6.18 \cdot 10^{-8}$
#15	-10.92	239.48	$5.58 \cdot 10^{-5}$	0.0265	9.178	0.382	$3.82 \cdot 10^{-7}$

4 Discussion

Against the backdrop of the ongoing global warming and enlargement of the areas with periglacial soil formation [19], the issues of seasonal transitions through zero degrees Celsius and associated frost heaving modify and, in cases of an increased volume of air voids, worsen the conditions of highway subsoils in the wintertime. Because of the potential complexity of soil conditions on-site and the practical issues when implementing field research, a laboratory-based approach using non-saline soil samples in an “open system” was developed. The significantly modified experimental design not only benefited from clear observation of temperature distributions and moisture transport over the sample length with time but also delivered a better understanding of mass moisture transfer in a vapour state at sub-zero temperatures. The maximum frost heave was observed at the freezing front of a 2 cm/day moving rate. Moreover, increased sample length signified the reduction of temperature drop near the transition zone next to the 0 °C isotherm. Such retardation of the freezing rate was necessary for the phase transition to occur and the heat balance to equilibrate or endeavor to do so. The moisture intake and its redistribution within the soil samples were also found to depend on the density and the chemical content of pore water. The total moisture intake in ice and unfrozen water, which was pulled up to the top 10 cm section, prevailed in a deionized water supply test.

There are not many works that have considered the gaseous component of mass transfer. The vapour flux has widely been omitted or underestimated by scientists in the calculation of mass transfer. One of the few works that have been considered was presented by [17].

The main distinctions and similarities of the current proposal with what they put forward are considered here:

1. In the current work, it is accepted that moisture mass transport is implemented primarily in the gas phase, i.e., vapour in the freezing fringe transport zone. Otherwise, it is supplied in the capillary zone from the water table source in a liquid state. Zhang et al. (2016) [17] accept the intake moisture flow as combined from liquid and water fluxes, conforming to thermal and isothermal hydraulic conductivities. The liquid water flow was presented by Richard's equation and explained as driven by water potential or temperature gradient, which is proportional to hydraulic conductivity.
2. In this work, it is assumed the vapour is fully saturated and filling all the volume of air voids in the soil. At the same time, Zhang et al. (2016) calculated the relative humidity H_r and vapour diffusivity D_a , including the empirical parameter of an enhancement factor η [17]. The vapour density was also found by the empirical formula of saturated vapour density multiplied by its relative humidity.
3. Zhang et al. (2016) determined the unfrozen water content in equation [17] by temperature, and the coefficients a and b were estimated by regression analysis of the measured data of temperature and unfrozen water content. However, it could be the case that " a " and " b " might vary for different types of soils. In Zhang et al.'s model, the presence of unfrozen water content in the frozen part of the soil was admitted. However, its mobility was considered doubtful and, hence, such water mass transfer was not accounted for unless it had evaporated and was transported in a gas state.
4. Zhang et al. (2016) simulated the natural field impacts of precipitation, evaporation and heat fluxes from the net radiation, which was omitted in the current study [17].
5. In this work, detailed positioning of the soil structure was considered, based on the experimental data of the measured temperature, vertical linear volumetric change registered by testing time and the obtained moisture-density relation.

The engineering properties of the samples after freeze-thaw cycles signified a clear reduction in strength, mainly because of increased moisture content and lowered dry density. The samples with loose density were compacted during the freeze-thaw cycles, while dense soils became loosened. It was observed that a shallow water table induced greater moisture intake to the soil samples and, consequently, their reduction in strength.

As many road subsoils are designed to be exploited in unsaturated conditions or undergo an unsaturated transition stage while being frozen (see Fig. 1), it is crucial to consider the moisture mass transfer in a gaseous state, accompanied by phase transitions. Building on the experimental results, the conceptual model for soil freezing was considered from the perspectives of moisture content, phase transfer and volume changes with temperature within the freezing soil. To determine the moisture mass transfer at different freezing stages, the degree of saturation and the voids ratio with time were set as the input parameters. Moisture mass transfer in the unsaturated freezing soils with a significant voids ratio was implemented predominantly with vapour flow. The concept of the moisture flows in gaseous state benefits from having a clear calculation algorithm, absence of empirical relations and compliance with the laws of physics. Vapour convection was naturally induced by the temperature gradient, where the driving force was presented by saturated vapour pressure difference with further energy release by the phase transfer in the frozen zone. This mode of moisture transfer is applicable for both saline and non-saline soils. Notably, the voids ratio and the moisture content have a significant impact on the mass transfer rate and ice growth. After the pore volume

is filled with ice, primarily deposited from the vapour, the further mass transfer has to be considered with hygroscopic water, which stays in a liquid state even at very low temperatures. The migration of the hygroscopic water is 175, explained as being driven to the frozen side by cryosection forces owing to a difference in surface tension.

Considered phenomenon of the vapour mass transfer and the interphase equilibrium in the freezing soils replicate with the many broader issues in the periglacial areas and help to explain many hitherto problems of moisture mass transfer occurring in the freezing soils.

5 Conclusions

Further outcomes have been concluded from the conducted work:

1. The significantly modified testing method, including the slow freezing techniques and longer samples lengths, is an effective way to evaluate the impact of freeze-thaw cycles on soils.
2. The obtained results have improved understanding of the heat and mass transfer phenomenon during the unidirectional freezing of soils.
3. The conceptual model for frost heave in soils was developed based on the vapour mass transfer. The algorithm of vapour flow calculation in unsaturated soils was presented using fundamental thermodynamic equations.
4. Temperature redistribution during the freeze-thaw tests of the samples with variable density between the columns did not have an obvious pattern regarding the temperature field. Such a feature can be explained by the slow freezing technique, which provided sufficient time for uniform freezing regardless of the soil density.
5. Observation of the temperature distribution revealed a reduction of temperature change in the transition zone next to the 0 °C isotherm. While the cooling rate was set to be stable, at 2 °C per day, the temperature drop over the soil length and the resulting frost heave were varied. The maximum frost heave was observed when the freezing rate over the sample length was 2 cm/day. A slow freezing rate was observed in the top 10–15 cm layer, and the boosted freezing was registered in the lower part of the soil samples.
6. Low-density soil samples contributed moisture mass transfer, while increased bulk density, in contrast, decelerated the passage of water. In addition, ice lens formation in the freezing front was prevalent in dense soils free of chemical content, while moisture absorption from the water table predominated in loose soils.

5.1 Key Limitations

A potential limitation in the data is due to the design of the experiment, particularly not being able to extract geotechnical samples below 0 °C. However, as the focus was on the overall impact of freeze-thaw on moisture transport, the overall conclusions are considered to be sound. The total moisture distribution in ice and unfrozen water could not be monitored over the sample lengths with respect to the testing time. As a result, the conclusions are based on the total net moisture transfer measured at the end of each test. It should be noted that these limitations do not detract from the scientific contribution of the work, where vapour flow was identified as a key source for moisture mass transfer.

5.2 Further Research Perspectives of Mass Transfer in the Freezing Soils

According to the findings of the research, the integrated moisture mass transfer in sub-zero temperatures includes moisture transport in a gaseous flow and hygroscopic water transfer in a liquid state, which in turn, depends on the surface tension and the cryosection forces. Consequently, both vapour mass transfer and associated phase transitions need to be taken into account. That is, only after taking into consideration both components of moisture flow and understanding its driving forces will it be possible to move to a new stage of the moisture mass transfer theory. Further research could include vapour mass transfer in quantitative analysis for different types of soils, taking into account the freezing rates, volumetric-moisture characteristics and particle size scenarios. The available techniques need to be reviewed and expressed with formulae explaining the driving force of hygroscopic water transport and vapour transport capacity. Special attention should be given to vapour mass transfer under highways. Application of the dynamic load, causing repeated short-term pressure increases and accompanying phase transition, would have an effect on the volumetric variations, and this needs to be considered in conjunction with site observations. Regarding laboratory experiments, installation of pore pressure probes and equipment sets for determining the voids ratio and moisture content, measured by sample length and recorded hourly, would benefit the calculations of the total flow of moisture with time. It is also important to consider the measurement and monitoring of hygroscopic moisture transport in relation to the testing time. The knowledge of the displacement of this component could entirely solve the problem of integrated moisture mass transfer in soils under sub-freezing temperatures. The presented vapour flow model is suitable for implementation with numerical analysis, including the finite element method, finite volume method, among others, where the mass of built ice can be calculated from the deposited vapour over time, according to the temperature in each mesh, separately and further integrated into the continuous flow. Determination of the hygroscopic moisture is feasible as the difference of the total mass transfer and vapour flow. Application of the presented method would benefit the accuracy of frost heave prognosis by fostering understanding of soil degradation, in particular, in highways subsoils.

References

1. Simonsen, E., Isacsson, U.: Soil behavior during freezing and thawing using variable and constant confining pressure triaxial tests. *Can. Geotech. J.* **38**(4), 863–875 (2001)
2. Han, C., Jia, Y., Cheng, P., Ren, G., He, D.: Automatic measurement of highway subgrade temperature fields in cold areas. In: 2010 International Conference on Intelligent System Design and Engineering Application (ISDEA), pp. 409–412 (2010)
3. Sarsembayeva, A., Zhussupbekov, A.: Experimental study of deicing chemical redistribution and moisture mass transfer in highway subsoils during the unidirectional freezing. *Transp. Geotech.* **26**, 100426 (2021)
4. Arenson, L.U., Sego, D.C., Newman, G.: The use of a convective heat flow model in road designs for Northern regions, pp. 1–8. IEEE (2006)
5. Zhang, J., Li, J., Quan, X.: Thermal stability analysis under embankment with asphalt pavement and cement pavement in permafrost regions. *Sci. World J.* **2013** (2013). Article ID: 549623

6. Sakanov, D.K.: Regional specific features of temperature mode of the road constructions Cand. in techn. sci. Kazakh academy of transport and communication named after M. Tynyshbayev (2007)
7. Teltayev, B.B., Loprencipe, G., Bonin, G., Suppes, E.A., Tileu, K.: Temperature and moisture in highways in different climatic regions. *Magazine of Civil Engineering* **100**(8), 10011 (2020)
8. Lai, Y., Pei, W., Zhang, M., Zhou, J.: Study on theory model of hydro-thermal-mechanical interaction process in saturated freezing silty soil. *Int. J. Heat Mass Transf.* **78**, 805–819 (2014)
9. Hermansson, Å.: Laboratory and field testing on rate of frost heave versus heat extraction. *Cold Reg. Sci. Technol.* **38**(2–3), 137–151 (2004)
10. Nagare, R., Schincariol, R., Quinton, W., Hayashi, M.: Effects of freezing on soil temperature, freezing front propagation and moisture redistribution in peat: laboratory investigations. *Hydrol. Earth Syst. Sci.* **16**(2), 501–515 (2012)
11. Bi, G.: Study on influence of freeze-thaw cycles on the physical-mechanical properties of loess. In: *Smart Materials and Intelligent Systems*, vol. 442, pp. 286–290 (2012)
12. Bing, H., He, P.: Experimental investigations on the influence of cyclical freezing and thawing on physical and mechanical properties of saline soil. *Environ. Earth Sci.* **64**(2), 431–436 (2011). <https://doi.org/10.1007/s12665-010-0858-y>
13. Ming, F., Li, D.: Experimental and theoretical investigations on frost heave in porous media. *Math. Probl. Eng.* (2015). Article ID: 198986. <https://doi.org/10.1155/2015/19898>
14. Wu, D., Lai, Y., Zhang, M.: Heat and mass transfer effects of ice growth mechanisms in a fully saturated soil. *Int. J. Heat Mass Transf.* **86**, 699–709 (2015)
15. Cui, Z., Zhang, Z.: Comparison of dynamic characteristics of the silty clay before and after freezing and thawing under the subway vibration loading. *Cold Reg. Sci. Technol.* **119**, 29–36 (2015)
16. Sinitsyn, A.O., Løset, S.: Strength of frozen saline silt under triaxial compression with high strain rate. *Soil Mech. Found. Eng.* **48**(5), 196–202 (2011). <https://doi.org/10.1007/s11204-011-9148-2>
17. Zhang, M., Wen, Z., Xue, K., Chen, L., Li, D.: A coupled model for liquid water, water vapor and heat transport of saturated-unsaturated soil in cold regions: model formulation and verification. *Environ. Earth Sci.* **75**(8), 1–19 (2016). <https://doi.org/10.1007/s12665-016-5499-3>
18. Zhussupbekov, A., Alibekova, N., Akhazhanov, S., Sarsembayeva, A.: Development of a unified geotechnical database and data processing on the example of Nur-Sultan City. *Appl. Sci.* **11**(1), 1–20, 306 (2021)
19. Harris, C., et al.: Permafrost and climate in Europe: monitoring and modelling thermal, geomorphological and geotechnical responses. *Earth Sci. Rev.* **92**, 117–171 (2009)